



Published in final edited form as:

*Bioconjug Chem.* 2007 ; 18(6): 2159–2168. doi:10.1021/bc700233w.

## Metallo-Phthalocyanine Near-IR Fluorophores: Oligonucleotide Conjugates and Their Applications in PCR Assays

Irina V. Nesterova<sup>†</sup>, Vera T. Verdree<sup>†</sup>, Serhii Pakhomov<sup>†</sup>, Karen L. Strickler<sup>†</sup>, Michael W. Allen<sup>||</sup>, Robert P. Hammer<sup>†</sup>, and Steven A. Soper<sup>\*,†,§</sup>

Department of Chemistry, Louisiana State University, Baton Rouge, Louisiana 70803, Department of Mechanical Engineering, Louisiana State University, Baton Rouge, Louisiana 70803, Center for BioModular Multi-Scale Systems, Louisiana State University, Baton Rouge, Louisiana 70803, and Thermo Electron Corporation, 5225 Verona Road, Madison, Wisconsin 52711

### Abstract

Water soluble, metallo-phthalocyanine (MPc) near-IR fluorophores were designed, synthesized, and evaluated as highly stable and sensitive reporters for fluorescence assays. Their conjugation to oligonucleotides was achieved via succinimidyl ester-amino coupling chemistry with the conditions for conjugation extensively examined and optimized. In addition, various conjugate purification and isolation techniques were evaluated as well. Results showed that under proper conditions and following purification using reverse-phase ion-pair chromatography, labeling efficiencies near 80% could be achieved using ZnPc (Zn phthalocyanine) as the labeling fluorophore. Absorption and fluorescence spectra accumulated for the conjugates indicated that the intrinsic fluorescence properties of the MPc's were not significantly altered by covalent attachment to oligonucleotides. As an example of the utility of MPc reporters, we used the MPc-oligonucleotide conjugates as primers for PCR (polymerase chain reaction) amplifications with the products sorted via electrophoresis and detected using near-IR fluorescence ( $\lambda_{\text{ex}} = 680 \text{ nm}$ ). The MPc dyes were found to be more chemically stable under typical thermal cycling conditions used for PCR compared to the carbocyanine-based near-IR reporter systems typically used and produced single and narrow bands in the electrophoretic traces, indicative of producing a single PCR product during amplification.

### INTRODUCTION

Because of a number of compelling advantages associated with near-IR fluorescence ( $\lambda > 650 \text{ nm}$ ), such as low scattering cross sections, reduced autofluorescence, lower radiation energy, and readily available diode lasers as excitation sources, it can provide better overall detection sensitivity compared to the visible and/or UV regions of the electromagnetic spectrum using rather simple instrumentation, especially when analyzing complex biological systems (1–3). Applications where the viability of near-IR fluorescence has been

\*Corresponding author. Phone: 225-578-1527. Fax: 225-578-3458. chsoper@lsu.edu.

<sup>†</sup>Department of Chemistry, Louisiana State University.

<sup>‡</sup>Department of Mechanical Engineering, Louisiana State University.

<sup>§</sup>Center for BioModular Multi-Scale Systems, Louisiana State University.

<sup>||</sup>Thermo Electron Corporation.

Supporting Information Available: HPLC separation of ZnPc **1** and conjugate **1-C12-O1**, procedure used for calculation of labeling efficiency, multiple conjugation products and their separation, purification of conjugation reaction using G25 microspin columns, and purification of conjugation reaction using ethanol precipitation. This material available free of charge via the Internet at <http://pubs.acs.org>.

demonstrated include DNA sequencing (4–6), detecting DNA restriction fragments (7) and adducts (8), analysis of PCR products (9), DNA microarrays (10), mutation detection (11), enzymatic substrate monitoring (12), and various fluorescence resonance energy transfer (FRET)-based assays (11,13).

Unfortunately, hurdles still exist, hampering the widespread utilization of near-IR fluorescence. The primary challenge is the limited set of fluorophores available for deep-red excitation that possess favorable chemical and photophysical properties for applications requiring covalent or noncovalent labeling of targets. Despite the growing number of fluorophores that show absorbing properties in the near-IR (14,15), the demands of modern multiplexed, ultrasensitive analyses require the development of new bright fluors with the following properties: (a) a diverse range of photophysical and spectral characteristics that can be easily tuned; (b) good chemical, thermal, and light stability; (c) availability of a wide range of functional groups for covalent conjugation to a variety of targets; and (d) narrow emission envelopes to minimize spectral leakage into various detection channels required for spectral multiplexing.

Phthalocyanines (Pc's) and metallo-phthalocyanines (MPc's) are well-known near-IR absorbing/fluorescing dyes (16). Various MPc's have been extensively studied, and many display photophysical properties that are comparable or even superior to those of the most commonly used near-IR reporter systems. These properties include high extinction coefficients ( $>10^5 \text{ M}^{-1} \text{ cm}^{-1}$ ) (17,18), favorable fluorescence quantum yields ( $>0.6$ ) (19–21), excellent photostability with photobleaching quantum yields as low as  $10^{-7}$  (17,22,23), and good chemical and thermal stabilities. Another appealing feature of MPc's is that their photophysical properties can be tuned by simply varying peripheral substitution patterns around the macrocycle (17,22,24) and/or altering the identity of the metal center (25,26).

Covalent attachment of MPc's with various biomolecules that have been reported include those with nucleobases (27), oligonucleotides (28–31), proteins (23,32–35), peptides (36), or monoclonal antibodies (35,37–39) as targets. However, in spite of the impressive photophysical and spectral properties associated with these near-IR dye systems, the analytical utility of MPc's when covalently attached to biomolecular targets have not been extensively reported.

The first commercially available MPc-based reporters were SiPc's (La Jolla Blue), which contained axial polyethylene glycol ligands used to prevent self-aggregation and improve water solubility. Oligonucleotides conjugated to La Jolla Blue were utilized for homogeneous hybridization assays of DNA and RNA targets with the hybridions monitored via transient-state polarized fluorescence with a detection limit reported to be 1 fmol (28,29). Peng and co-workers (35) developed another SiPc dye with highly charged axial ligands, IRD700DX, and demonstrated its applicability as a bright and photostable near-IR fluorescent label (fluorescence quantum yield of 0.14 in PBS and photobleaching quantum yield of  $1.6 \times 10^{-7}$ ) for antibody conjugation.

Duan et al. (37) reported on the conjugation of ZnPc, which lacks axial ligands to the metal center, to monoclonal antibodies used to bind to cells bearing the relevant antigenic species. We have previously reported the design, synthesis, and conjugation of MPc's and naphthalocyanines to proteins and oligonucleotides in which two water-soluble asymmetric ZnPc- and naphthalo-cyanine-based near-IR labeling dyes with isothiocyanate functional groups were conjugated to primary amine-containing targets (30). Conjugates of a water soluble ZnPc (**2**, Scheme 1) to streptavidin were prepared and the properties of the conjugates studied (23).

The limited use of *Pc*-based labeling fluors have resulted from the lack of (a) appropriately designed molecules that are soluble, possess favorable photophysical properties in aqueous media, and bear functional groups for conjugation; (b) documented labeling conditions that result in the facile and high yield conjugation to biomolecules; and (c) simple and efficient purification protocols for isolating the conjugate.

Herein we report on two water-soluble MPc's, asymmetrical and symmetrical ZnPc's with no axial ligands (**1** and **2**, respectively, see Scheme 1), for conjugation to targets containing primary amine groups. To demonstrate the utility of these labeling fluorophores, the conditions for highly efficient labeling of oligonucleotide targets and robust approaches for the effective isolation and purification of the conjugates are provided as well as the spectral and photophysical properties of the conjugates. Finally, we evaluate the use of these ZnPc-oligonucleotide conjugates as primers for PCR amplifications as analyzed by the gel electrophoretic sorting of the generated amplicons with near-IR fluorescence detection.

## EXPERIMENTAL PROCEDURES

### Materials

All materials were of reagent grade and were purchased from commercial suppliers, such as Sigma-Aldrich, EMD or Fisher, and used as received unless otherwise noted. Anhydrous DMF (*N,N*-dimethylformamide) and ether were dried before use by passing through columns with molecular sieves and activated alumina. Milli Q water (18 m $\Omega$ ) produced in-house was used for all solution preparations. Oligonucleotide sequences modified with an amino group at their 5'-end via aliphatic (C<sub>6</sub>H<sub>12</sub> or C<sub>12</sub>H<sub>24</sub>) linkers or unmodified were obtained from IDT (Coralville, IA). Their sequences and melting temperatures ( $T_m$ ) for fully matched duplexes are listed in Table 1. Precast agarose gel plates (3%) were purchased from BioRad (Hercules, CA). dNTPs (deoxynucleotides triphosphates) and PCR buffers were purchased from Applied Biosystems (Foster City, CA).

### Synthesis of ZnPc's **1**, **2**, and Succinimidyl Ester **5** (Scheme 2)

The preparation of these compounds has been reported elsewhere (23,40).

### Synthesis of Succinimidyl Ester **3**

The synthesis of this compound was adapted from published procedures with slight modifications (41). A mixture of DCC (6 mg, 0.029 mM) and NHS (4 mg, 0.035 mM) was added to ZnPc **1** (12.6 mg, 0.010 mM) dissolved in anhydrous DMF (2 mL). The reaction was stirred for 18 h at room temperature in an argon atmosphere while protecting it from light. After the reaction, diethyl ether (approximately 20 mL) was added to the reaction mixture. The sample was centrifuged and the supernatant discarded. The residue was dissolved in acetone, filtered through a 0.2  $\mu$ m Teflon filter, and evaporated, which afforded 8 mg (59% yield) of succinimidyl ester **3** as a dark-blue powder. MS  $m/z$  ( $M + H^+$ ) 1296.481, calculated for C<sub>64</sub>H<sub>66</sub>N<sub>9</sub>O<sub>17</sub>Zn 1296.387.

### Synthesis of Succinimidyl Ester **4**

The synthesis of this compound was adapted from published procedures with slight modifications (41). A solution of ZnPc **2** (42 mg, 0.037 mmol), NHS (*N*-hydroxysuccinimide) (4.7 mg, 0.041 mmol), and DCC (*N,N'*-dicyclohexylcarbodiimide) (8.4 mg, 0.041 mmol) in anhydrous DMF (1.5 mL) was stirred at room temperature in an argon atmosphere for 60 h. The reaction mixture was filtered, the precipitate washed with DMF (5 mL), and the clear filtrate diluted with ether (70 mL) inducing precipitation of the product, which was then centrifuged and the supernatant discarded. The crude product was redissolved in DMF (3 mL) and reprecipitated with ether. After centrifugation, the product

was dried *in vacuo*, which afforded 25 mg (56% yield) of succinimidyl ester **4** as a dark-blue powder.  $^1\text{H NMR}$  (400 MHz, DMSO- $d_6$ )  $\delta$  9.10–8.80 (br. s, 4H), 8.75–8.40 (m, 4H), 8.37–8.18 (m, 2H), 8.20–8.00 (m, 6H), 7.90–7.74 (m, 4H), 7.70–7.35 (m, 8H), 2.92 (br. s, 4H). MS  $m/z$  1217.09, calcd for  $\text{C}_{64}\text{H}_{35}\text{N}_9\text{O}_{14}\text{Zn}$ , 1217.16.

### Oligonucleotide–ZnPc Conjugation Reactions

The labeling procedure used was adapted from Molecular Probe's (Carlsbad, CA) standard protocol for amino-reactive Alexa Fluor succinimidyl esters. Stock solutions of **3–5** (5–10 mM) were prepared in DMSO (dimethyl sulfoxide). Labeling buffers were prepared in-house by dissolving the appropriate amount of the corresponding salts in water and adjusting the pH using HCl and/or NaOH. The amino-modified oligonucleotide was purified by ethanol precipitation before the conjugation reaction to remove any amino-containing impurities. The purified oligonucleotide was redissolved in water to yield a solution with a concentration of  $\sim 25 \mu\text{g/mL}$  (5 mM).

Unless otherwise noted, the reaction mixture included (in order of addition) succinimidyl ester **3**, **4**, or **5** (200 nmol), water (7  $\mu\text{L}$ ), labeling buffer (75  $\mu\text{L}$ ), and oligonucleotide (20 nmol). The reaction was incubated at room temperature for 15–18 h. Labeled oligonucleotides were purified by ethanol precipitation (to partially remove excess unreacted dye) using 250  $\mu\text{L}$  of cold absolute ethanol and 10  $\mu\text{L}$  of 3 M NaCl added to the reaction mixture. The solutions were mixed and kept at  $-20^\circ\text{C}$  for 30–60 min and centrifuged at 12,000 rpm with the supernatant discarded. The precipitate was dried on air and reconstituted in 100  $\mu\text{L}$  of 0.1 M TEAA (triethylammonium acetate) for chromatographic analysis and purification. The isolated fractions were combined and concentrated in a rotary evaporator. The excess TEAA was removed by drying in high vacuum ( $<0.01 \text{ mmHg}$ ) at room temperature.

### High Performance Liquid Chromatography (HPLC)

The HPLC separations were performed using a JASCO (Easton, MD) 2000-series HPLC equipped with a quaternary gradient pump, autosampler, and fluorescence and diode-array detectors. The analytical column (Zorbax C18, 5  $\mu\text{m}$ , 4.6 mm  $\times$  150 mm) was purchased from Agilent Technologies (Santa Clara, CA). The following gradient was used (flow rate = 1.0 mL/min): initial hold at 95% 0.1 M TEAA/5% MeOH for 5 min; ramp up to 5% 0.1 M TEAA/95% MeOH in 30 min; hold for 5 min; and wash for 15 min with 100% MeOH at 1.5 mL/min. The column was allowed to equilibrate at the initial mobile phase conditions for 20 min before the next injection. Typically, two wavelengths were monitored using the diode-array detector: 260 and 680 nm. The fluorescence detector was set to an excitation wavelength of 677 nm, and the emission wavelength was set to 687 nm, the corresponding maxima for ZnPc **2** absorption and emission (23).

### Determination of Conjugate Concentrations

The concentrations of the ZnPc-labeled oligonucleotides were determined by HPLC against a calibration curve obtained using solutions of the corresponding ZnPc at various concentrations (0.5–100  $\mu\text{M}$ ) when monitoring absorption at 680 nm, where the oligonucleotide offered little if any absorption.

### Absorption and Fluorescence Measurements

All absorption spectra were acquired using an Ultrospec 4000 spectrophotometer (Pharmacia Amersham Biosciences, Piscataway, NJ) or Cary 50 UV&-vis (Varian, Palo Alto, CA) with 10 mm path length quartz cuvettes. Emission spectra were acquired using a FLUOROLOG-3 spectrofluorometer (Horiba Jobin Yvon, Edison, NJ) equipped with a 450

W xenon lamp and a cooled Hamamatsu R928 photomultiplier operated at 900 V in the photon-counting mode. All spectral measurements were performed under ambient conditions within 3 h of solution preparation.

### DNA Hybridization

The hybridization of conjugate **2-C6-O1** (here and elsewhere, **1** or **2** represents ZnPc label (Scheme 1, **1** or **2**); **C6** or **C12**, aliphatic linker containing 6 or 12 carbon atoms, respectively; **O1** or **O2**, oligonucleotide sequence (see Table 1)) with complement **O2** was performed by incubating 1  $\mu$ M solutions of both the labeled oligonucleotide (**2-C6-O1**) and its complement **O2** at equal molar concentrations in a buffer containing 10 mM Tris-HCl, 4 mM MgCl<sub>2</sub>, and 15 mM KCl at pH 8.5 for 2 h at 30 °C.

### Polymerase Chain Reactions (PCRs)

PCRs were performed on M13mp18 DNA (USB, Cleveland, OH) or human placental DNA (Sigma-Aldrich, St. Louis, MO) targets. PCR primers (see Table 1 for sequences) were designed to amplify 185 bp, 272 bp, and 381 bp regions of the M13mp18 DNA target and a 98 bp region of human placental DNA. PCRs were performed using a GeneAmp reagent kit with AmpliTaq DNA polymerase (Applied Biosystems, Foster City, CA). PCR cocktails consisted of 1  $\mu$ L of each of the primers (~1  $\mu$ M whenever known), 2  $\mu$ L of dNTPs (0.2 mM), 10  $\mu$ L of 10 $\times$  PCR buffer, 1  $\mu$ L of Taq DNA Polymerase (0.5 unit/ $\mu$ L), 1  $\mu$ L of DNA template (2 ng/ $\mu$ L), and 84  $\mu$ L of PCR qualified water. PCR was carried out using a commercial thermal cycling instrument (Eppendorf, Hamburg, Germany or Techne, Burlington, NJ). M13mp18 amplifications consisted of the following (30 cycles): 94 °C for 30 s; 57 °C for 40 s; 72 °C for 60 s; and a final extension at 72 °C followed by a cooling step at 4 °C. Thermal cycling of the human placental DNA was designed to amplify the CFTR (cystic fibrosis transmembrane conductance regulator) gene and consisted of an initial denaturation step at 94 °C for 5 min followed by (30 cycles) 94 °C for 40 s; 62 °C for 40 s; 72 °C for 60 s; and a final extension at 72 °C followed by a cooling step to 4 °C. PCRs were also conducted using unlabeled primers of the same sequence as those of the labeled primers to evaluate PCR performance in the presence of the MPc dye reporter.

### Gel Electrophoresis

PCR products were electrophoresed either in a 3% precast agarose gel (Bio-Rad Laboratories, Hercules, CA) or a 5.5% (w/v) cross-linked polyacrylamide gel (Li-COR Biosciences, Lincoln, Nebraska). For the agarose gel, separation was performed at 140 mV in 1  $\times$  TAE buffer (Bio-Rad Laboratories, Hercules, CA). Amplicons were indexed against a DNA sizing ladder (50–1000 bp, Promega, Madison, WI). After separation, the gels were stained with ethidium bromide (~0.3  $\mu$ L/mL), and images were collected using a Logic Gel imaging system (Eastman Kodak Company, Rochester, NY).

The polyacrylamide gel was polymerized between two borofloat glass plates (21 cm  $\times$  25 cm) and placed in the Global IR<sup>2</sup>DNA analysis system (Li-COR Biosciences, Lincoln, NE). The electrophoresis was typically run at 1,500 V for 2.5 h. Amplicons were indexed against a 50–350 bp IRD700-labeled size standard (Li-COR Biosciences, Lincoln, NE). The fluorescence detector contained in this instrument consisted of a scanning laser ( $\lambda$  = 680 nm), an avalanche photodiode detector, and a bandpass filter (preset center wavelength = 720 nm; pass band ~20 nm) situated in front of this detector to isolate the monitored fluorescence.

## RESULTS AND DISCUSSION

ZnPc's **1** and **2** (asymmetrical and symmetrical, respectively; see Scheme 1) possess photophysical properties that are comparable or superior to those of commercially available near-IR dyes (e.g., ZnPc **2**: extinction coefficient =  $2.9 \times 10^5$ , fluorescence quantum yield = 0.41, and photobleaching quantum yield =  $5.0 \times 10^{-7}$ ; commercially available near-IR dye IRD700: fluorescence quantum yield = 0.70; photobleaching quantum yield =  $4.6 \times 10^{-6}$  (23)), are chemically, thermally, and light stable, and are fairly water-soluble, which was achieved by decorating the macrocycle periphery with polar solubilizing groups (triethylene glycols (TEG) or carboxylates). These ZnPc's have narrower absorption and emission envelopes compared to those of the carbocyanine-based near-IR dyes (see Figure 1), making them particularly attractive for spectral multiplexing applications. Additionally, these dyes contained at least one carboxylic group, a convenient and common functionality that can be used for robust labeling of amino-modified biomolecules such as oligonucleotides via succinimidyl ester chemistry (43).

Two types of MPc's were evaluated in this study: an asymmetric ZnPc **1** containing three triethylene glycol groups to provide solubility in aqueous media and a functional carboxylic group that could be used for labeling reactions, and a symmetric ZnPc **2**, which contained four carboxylic groups that provided both solubilization of the dye in aqueous media and a functional handle to covalently attach the fluorophore to a target.

### Conjugation Reactions

The use of succinimidyl esters and their reaction with primary amines has been reported for several MPc's (28,29,31). We applied this coupling approach to amino-modified oligonucleotides, and ZnPc's **1** and **2** converted into succinimidyl esters **3–5** (see Scheme 2). The conjugates, **1-C12-O1**, **2-C12-O1**, and **1-C6-O1**, were isolated using ion-pair reverse-phase chromatography. The chromatographic separation was achieved using a 0.1 M TEAA/CH<sub>3</sub>OH gradient (see Figure 2a and Figure S1 in Supporting Information). Using similar gradients with CH<sub>3</sub>CN rather than CH<sub>3</sub>OH did not result in complete separation of the labeled conjugates from excesses of the corresponding MPc's.

As a control, it was necessary to demonstrate that conjugations were not simply noncovalent associations between the MPc dye and the oligonucleotide. To verify this, a reaction involving a nonreactive MPc (carboxylic acid **2** instead of succinimidyl ester **4** or **5**) and the amino-modified oligonucleotide **O1** was conducted. Inspection of the control chromatograms (Figure 2b) showed no evidence of the MPc's nonspecifically associating with the oligonucleotides; no peak for an association complex was detected in the chromatographic trace. Similar data was also obtained for PEG-modified ZnPc **1** (data not shown).

Experiments were then conducted to optimize the extent of the conjugation reaction by altering reaction conditions, such as pH, buffer composition, and the dye-to-oligonucleotide molar ratio. The labeling efficiencies were evaluated by monitoring the decrease in the original oligonucleotide content observed from the chromatographic traces (details are included in the Supporting Information; see Figure S2). The labeling efficiencies were estimated for various conditions, the results of which are summarized in Tables 2 and 3.

For molecules containing more than one carboxylic group (e.g., ZnPc **2**), several types of succinimidyl esters with different numbers of carboxylic groups converted to succinimidyl esters were possible. Two activated esters of ZnPc **2** were obtained and used for the labeling evaluation: the tetra-succinimidyl ester **5** (all four carboxylic groups are converted to the succinimidyl esters) and the monosuccinimidyl ester **4** (only one carboxylic group is

converted to the succinimidyl ester). As seen in Table 2, tetra-succinimidyl ester **5** resulted in better labeling efficiencies (78%) compared to that of the monosuccinimidyl ester **4** (53%) when using an MPc/oligonucleotide molar ratio of 11:1. This may have resulted from a higher effective concentration of the succinimidyl ester groups associated with the tetra-succinimidyl ester **5** compared to that of the monosuccinimidyl ester **4**. However, multiple targets may become attached to the same fluorophore when using labeling fluors that have several functional groups, as in the case of tetra-ester **5** compared to the monoester **4**, which can complicate the purification step. Indeed, multiple products were observed in the chromatogram when the succinimidyl ester **5** was used. At least two products were observed in the chromatogram when an 11-fold molar excess of the ester was used (see Figure S3 in Supporting Information), one which could be ascribed to the 1:1 MPc/oligonucleotide conjugate and another to a conjugate in which two oligonucleotides were linked to the same dye. The use of molar excesses below 11:1 (MPc/oligonucleotide) when using succinimidyl ester **5** yielded appreciable levels of the tri- and tetra-substituted products (data not shown).

It was generally observed that the labeling efficiency improved with increases in the MPc-to-oligonucleotide molar concentration ratio up to 11:1 (see Table 2), irrespective of the identity of the dye or succinimidyl ester used. The use of an excess of succinimidyl ester was necessary to overcome competing hydrolysis reactions of these functional groups. However, increasing the MPc/oligonucleotide molar ratio beyond approximately 11:1 reduced the extent of labeling (see Table 2). For example, succinimidyl ester **5** showed decreases in the reaction yield from 78% to 39% when the MPc/oligonucleotide molar ratio changed from 11:1 to 38:1, respectively. At higher dye concentrations, aggregation effects between MPc dyes began to dominate (44), which reduced the number of monomeric molecules available for the conjugation reaction. Thus, an MPc/oligo molar concentration ratio of approximately 10:1 was found to be optimal for these conjugation reactions.

We also investigated the effect of different aliphatic linker lengths used to tether the functional group (i.e., primary amine) to the oligonucleotide on the MPc-oligonucleotide labeling efficiency. As noted for ZnPc **2** and the monosuccinimidyl ester **4** (see Table 2), better overall labeling efficiencies were observed for oligonucleotides containing a C<sub>12</sub>H<sub>24</sub> linker compared to those with C<sub>6</sub>H<sub>12</sub> linkers. The improved labeling efficiency for the C<sub>12</sub>H<sub>24</sub> linker may be explained by reductions in electrostatic interactions between the anionic MPc and oligonucleotides when compared to that in the C<sub>6</sub>H<sub>12</sub> linker.

Various buffer compositions and pH values were also investigated as to their effects on the extent of labeling oligonucleotides with these ZnPc dyes. Inspection of Table 3 shows that for the labeling conditions tested (C<sub>6</sub>H<sub>12</sub> linker, ZnPc **2**, succinimidyl ester **4**, and MPc/oligonucleotide molar ratio of 9:1), better labeling was achieved at pH 7.5 when using the carbonate buffer (67%), while for the borate buffer, higher labeling efficiencies were obtained at a pH value of 8.5 (38%). It was also observed that at all pH values, carbonate buffers yielded higher labeling efficiencies. The effects of pH on labeling efficiency most likely resulted from the necessary balance between three factors: succinimidyl ester group hydrolysis rate, amine group reactivity, and solubility of **1** and **2** in aqueous media. All of these parameters are known to increase with increasing pH (43). The enhancement of the labeling efficiency when carbonate buffer was used compared to that with borate (59% vs 38% at pH 8.5; see Table 3) agreed with similar observations reported in the literature using succinimidyl chemistry (45).

### Conjugate Purification and Isolation

The standard protocols used to purify oligonucleotides from low molecular weight components, SEC filtration, ethanol precipitation, and HPLC, were evaluated for the isolation of MPc-oligonucleotide conjugates. Sephadex G25 size-exclusion columns were

found to retain not only ZnPc **2** but also conjugate **2-C6-O1** (see HPLC traces in Figure S4 in Supporting Information), indicating that the separation was not exclusively based on size but also partially on interactions of the dye with the solid support. Ethanol precipitation, an approach based on the limited solubility of oligonucleotides in cold ethanol, also did not provide adequate purification of the conjugates to allow it to be used exclusively. ZnPc's **1** and **2** have limited solubility in EtOH, which results in only ~40% of the unreacted dye being removed in the ethanol supernatant (see HPLC traces in Figure S5 in Supporting Information). A combination of ethanol precipitation followed by reverse-phase ion pair chromatography was found to give the most efficient isolation/purification approach for the MPc–oligonucleotide conjugates. It allowed for pure conjugates to be isolated, even when 10-fold molar excesses of the dye were used; no residual MPc's and/or unlabeled oligonucleotide were observed in chromatograms of the isolated conjugates when subjected to a preclean-up with cold ethanol followed by reverse-phase chromatography (data now shown).

### Spectral Properties of the MPc–Oligonucleotide Conjugates

Electronic absorption spectra of the conjugate **2-C12-O1** (Figure 3a) contained features characteristic of both domains, MPc and the oligonucleotide, including absorption bands at ~360 and 680 nm associated with the ZnPc and strong absorption between 250 and 260 nm indicating the presence of the oligonucleotide. Also, strong fluorescence was observed around 690 nm from the ZnPc moiety. The fluorescence emission profiles of the isolated conjugates and the corresponding MPc's were similar with no spectral feature changes observed in the conjugates compared to the corresponding ZnPc dyes (see Figure 3b).

One of the important intrinsic properties of *Pc*'s and MPc's is their high propensity to aggregate in aqueous solutions (21,26) with dimerization constants as high as  $10^{-9} \text{ M}^{-1}$  (46). With very few exceptions, neither MPc dimers nor higher order cofacial aggregates fluoresce (47–49). Electronic adsorption spectra of MPc's can provide insight into ground-state aggregation processes (50); a split and blue-shifted Q-band typically indicates cofacial ground-state aggregation of *Pc* rings (19,44,46,51,52). Both the free ZnPc **2** and its conjugate **2-C12-O1** showed various degrees of ground-state aggregation in aqueous media as noted from blue-shifts in the absorption maximum, generating a broadband as compared to the molecule in DMSO, where aggregation is expected to be minimal (see Figure 3a).

The absorption spectra of **2-C6-O1** and **2-C6-O1** hybridized to a 42-bp complement oligonucleotide **O2** (see Table 1) were also interrogated. The electronic absorption spectra (Figure 4a) indicated almost complete aggregation of ZnPc **2**, partial aggregation of conjugate **2-C6-O1**, and significant reductions in aggregation for the hybrid of **2-C6-O1** with **O2**. The fluorescence results correlated well with the adsorption spectra (see Figure 4b); no detectable fluorescence was observed for ZnPc **2** with a 13-fold increase in fluorescence for the **2-C6-O1/O2** hybrid compared to that for **2-C6-O1** alone. These results indicate that MPc aggregation can be substantially diminished when the MPc reporter is part of relatively large oligonucleotide constructs. Similar phenomena have been observed for MPc aggregation upon conjugation to monoclonal antibodies (37). However, for the tricyanocyanine near-IR dyes, complete deaggregation effects were observed when this dye was attached to a single nucleotide base (53) consistent with the fact that the carbocyanines have low aggregation propensities compared to those of the MPc-based dye systems.

### PCR-Based Applications

The ZnPc–oligonucleotide conjugates were next evaluated as potential reagents/reporters for PCR by amplifying different sized regions of an M13mp18 DNA template and a 98 bp region of the exon-10 CFTR gene containing the  $\delta F508$  mutation, which can provide a high

diagnostic value for cystic fibrosis (54). The amplicons were sorted by gel electrophoresis using either an agarose gel with UV detection after staining with ethidium bromide or a polyacrylamide gel with near-IR fluorescence detection at ~700 nm.

A comparison of the chemical/thermal stability of ZnPc- and carbocyanine-based near-IR fluorophores was first investigated using PCR, which contained all reagents except the amplification target and polymerase, and was carried through typical thermal cycling conditions. The results of this investigation are shown in Figure 5. (The fluorescence measurements were performed at room temperature following thermal cycling.) As can be seen in the results in Figure 5, the emission intensities for the carbocyanine-labeled oligonucleotide showed incremental decreases with increasing thermal cycle number, while the ZnPc **2** reporter showed modest increases in its fluorescence intensity with increasing thermal cycle number. The loss in fluorescence intensity for the carbocyanine is indicative of chemical changes in the chromophore induced by thermally activated reactions, which result in decreases in the fluorescence of this molecule. In the case of ZnPc **2**, no such reactions were found to occur at the conditions used herein. We also note that the slight increases in the fluorescence observed for the ZnPc **2** chromophore as a function of cycle number could have resulted from deaggregation of the ZnPc-oligonucleotide conjugate (see results in Figures 3 and 4).

We next performed PCR amplification of an M13mp18 or human genomic DNA target using the ZnPc **1** (asymmetrical) and **2** (symmetrical) reporter dyes. The size of the PCR amplicons obtained using both *Pc*-based dye/oligonucleotide conjugates correlated well with their expected sizes based on the known sequences of the test templates and the primer sequences when referenced against standard DNA ladders (see Figure 6). Another important conclusion is that no erroneous bands were detected in either of the PCRs, indicating that the ZnPc-based fluorophores did not perturb the PCR process. The results in Figure 6a show agarose gel electropherograms of PCR amplicons (381 bp) generated using **1**- and **2**-labeled primers or an unlabeled DNA primer. Qualitatively, the correct amplicons were generated for PCRs using the MPC-labeled primers when compared to the same PCRs using the unlabeled primers based on product size.

From the polyacrylamide gel electropherogram shown in Figure 6b, single bands were observed irrespective of amplicon size (185 or 272 bp) with similar amplicon yields using either **1** or **2** as the fluorescent label. The lack of smearing in the electrophoretic bands or the presence of phantom bands indicated that the dye-oligonucleotide constructs did not interact due to dye/dye-induced aggregation to either the amplicons or unconsumed primers following PCR.

As a demonstration of the ability to use these labels for the analysis of PCR products with diagnostic value, human genomic DNA was amplified using primers specific for exon-10 of the CFTR gene, which contains a mutation that provides molecular diagnostic information for cystic fibrosis. As can be seen from the image displayed in Figure 6c, 98 bp amplicons were clearly visible. It should be noted that the fluorescence detector used in this electrophoresis unit was not optimized for the MPC dye systems; the filter system installed in the instrument was designed for dicarbocyanine dyes, which have comparatively larger Stoke's shifts and broader excitation/emission envelopes compared to those of the ZnPc dyes (see Figure 1).

## CONCLUSIONS

ZnPc's **1** and **2** (asymmetrical and symmetrical, respectively) were designed to provide water solubility and carboxylic groups that could be used for labeling biomolecules through

succinimide-based chemistry. The ZnPc's afforded labeling efficiencies of 80% of target oligonucleotides using optimized conditions, including proper pH (7.5), buffer composition (carbonate), linker structure (C<sub>12</sub>H<sub>24</sub>), and stoichiometry between the MPc and oligonucleotide (~10:1, respectively). In addition, facile purification strategies were reported on the basis of ion-pair reverse-phase chromatography preceded by cold ethanol precipitation.

Spectroscopic investigations indicated that the conjugation of ZnPc's **1** and **2** to oligonucleotides did not alter their intrinsic fluorescence emission properties but affected the aggregation properties of the MPc's when placed in aqueous media. Partial deaggregation of ZnPc **2** was observed when this dye was attached to a 17mer oligonucleotide as revealed from its ground-state spectrum with slight fluorescence noted for the conjugate compared to that for the native dye in aqueous buffer. When the conjugate was hybridized to its complement, creating a double-stranded 42mer, a 13-fold increase in the fluorescence was observed compared to that in the dye/17mer construct. Because most molecular biology applications, such as PCR and cycle sequencing, create constructs that are larger than the starting primer and the primers are used in large molar excesses, this property could potentially reduce interferences from unextended primers when fluorescence is used for readout.

Another attractive feature of the MPc dyes compared to other near-IR dyes is their superior thermal/chemical stability. These features along with their outstanding photostability (photo-bleaching quantum yield of  $5 \times 10^{-7}$  (23)), narrow absorption/emission envelopes (see Figure 1), and near-IR excitation/emission properties will make *Pc* dyes very attractive candidates for a variety of highly sensitive and multiplexed biomolecular applications (55).

## Supplementary Material

Refer to Web version on PubMed Central for supplementary material.

## Acknowledgments

We thank the National Institutes of Health (National Human Genome Research Institute, Grants HG001499 and CA099246), the National Science Foundation (Grant Numbers CHE-0304833 and EPS-0346411), and the Louisiana Board of Regents for the financial support of this work.

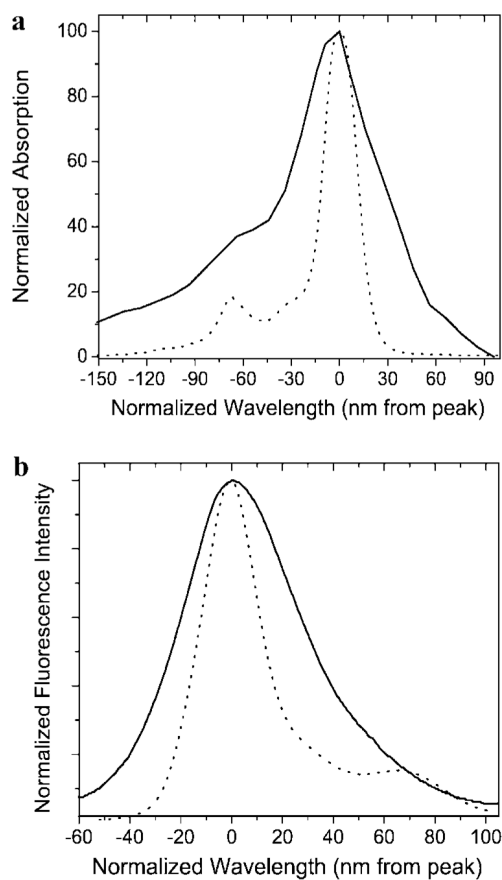
## LITERATURE CITED

1. Williams DC, Soper SA. Ultrasensitive near-Ir Fluorescence Detection for Capillary Gel-Electrophoresis and DNA-Sequencing Applications. *Anal Chem* 1995;67:3427–3432. [PubMed: 8686892]
2. Soper SA, Mattingly QL. Steady-State and Picosecond Laser Fluorescence Studies of Nonradiative Pathways in Tricarbocyanine Dyes - Implications to the Design of near-Ir Fluorochromes with High Fluorescence Efficiencies. *J Am Chem Soc* 1994;116:3744–3752.
3. Soper SA, Mattingly QL, Vegunta P. Photon Burst Detection of Single near-Infrared Fluorescent Molecules. *Anal Chem* 1993;65:740–747.
4. McWhorter S, Soper SA. Near-infrared laser-induced fluorescence detection in capillary electrophoresis. *Electrophoresis* 2000;21:1267–1280. [PubMed: 10826670]
5. Zhu L, Stryjewski W, Lassiter S, Soper SA. Fluorescence multiplexing with time-resolved and spectral discrimination using a near-IR detector. *Anal Chem* 2003;75:2280–2291. [PubMed: 12918968]
6. Lassiter SJ, Stryjewski WJ, Wang Y, Soper SA. Shedding light on DNA analysis - Multiplexed detection and identification using fluorescence lifetime methods. *Spectroscopy* 2002;17:14–23.

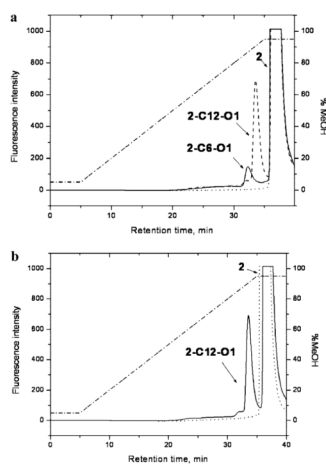
7. Owens CV, Davidson YY, Kar S, Soper SA. High resolution separation of DNA restriction fragments using capillary electrophoresis with near-IR, diode-based, laser-induced fluorescence detection. *Anal Chem* 1997;69:1256–1261.
8. Li GD, Gao JX, Zhou XJ, Shimelis O, Giese RW. Handling and detection of 25 amol of near-infrared dye deoxynucleotide conjugates by capillary electrophoresis with laser-induced fluorescence detection. *J Chromatogr A* 2003;1004:47–50. [PubMed: 12929960]
9. Peter C, Meusel M, Grawe F, Katerkamp A, Cammann K, Borchers T. Optical DNA-sensor chip for real-time detection of hybridization events. *Fresenius' J Anal Chem* 2001;371:120–127. [PubMed: 11678181]
10. Lassiter SJ, Stryjewski W, Legendre BJ, Erdmann R, Wahl M, Wurm J, Peterson R, Middendorf L, Soper SA. Time resolved fluorescence imaging of slab gels for lifetime base-calling in DNA sequencing applications. *Anal Chem* 2000;72:5373–5382. [PubMed: 11080890]
11. Wabuyele MB, Farquar H, Stryjewski W, Hammer RP, Soper SA, Cheng YW, Barany F. Approaching real-time molecular diagnostics: Single-pair fluorescence resonance energy transfer (spFRET) detection for the analysis of low abundant point mutations in K-ras oncogenes. *J Am Chem Soc* 2003;125:6937–6945. [PubMed: 12783546]
12. Chen XL, Li DH, Yang HH, Zhu QZ, Zheng H, Xu JG. A new red-region substrate, tetra-substituted amino aluminium phthalocyanine, for the fluorimetric determination of H<sub>2</sub>O<sub>2</sub> catalyzed by mimetic peroxidases. *Analyst* 2001;126:523–527. [PubMed: 11340992]
13. Kurner JM, Klimant I, Krause C, Pringsheim E, Wolfbeis OS. A new type of phosphorescent nanospheres for use in advanced time-resolved multiplexed bioassays. *Anal Biochem* 2001;297:32–41. [PubMed: 11567525]
14. Kricka LJ. Stains, labels and detection strategies for nucleic acids assays. *Ann Clin Biochem* 2002;39:114–129. [PubMed: 11928759]
15. Gomez-Hens A, Aguilar-Caballo MP. Long-wavelength fluorophores: new trends in their analytical use. *TrAC, Trends Anal Chem* 2004;23:127–136.
16. Fabian J, Nakazumi H, Matsuoka M. Near-Infrared Absorbing Dyes. *Chem Rev* 1992;92:1197–1226.
17. Ogunsipe A, Chen JY, Nyokong T. Photophysical and photochemical studies of zinc(II) phthalocyanine derivatives - effects of substituents and solvents. *New J Chem* 2004;28:822–827.
18. Kobayashi N, Ogata H, Nonaka N, Luk'yanets EA. Effect of peripheral substitution on the electronic absorption and fluorescence spectra of metal-free and zinc phthalocyanines. *Chem-Eur J* 2003;9:5123–5134.
19. Dhami S, Phillips D. Comparison of the photophysics of an aggregating and non-aggregating aluminium phthalocyanine system incorporated into unilamellar vesicles. *J Photochem Photobiol, A* 1996;100:77–84.
20. Ambroz M, Beeby A, MacRobert AJ, Simpson MSC, Svendsen RK, Phillips D. Preparative, Analytical and Fluorescence Spectroscopic Studies of Sulfonated Aluminum Phthalocyanine Photosensitizers. *J Photochem Photobiol, B* 1991;9:87–95. [PubMed: 1907646]
21. Kobayashi N, Higashi R, Ishii K, Hatsusaka K, Ohta K. Aggregation, complexation with guest molecules, and mesomorphism of amphiphilic phthalocyanines having four- or eight tri(ethylene oxide) chains. *Bull Chem Soc Jpn* 1999;72:1263–1271.
22. Ogunsipe A, Nyokong T. Effects of substituents and solvents on the photochemical properties of zinc phthalocyanine complexes and their protonated derivatives. *J Mol Struct* 2004;689:89–97.
23. Verdree VT, Pakhomov S, Su G, Allen MW, Countryman AC, Hammer RP, Soper SA. Water soluble metallo-phthalocyanines: the role of the functional groups on the spectral and photophysical properties. *J Fluoresc* 2007;17:547–563. [PubMed: 17574523]
24. Cook MJ, Dunn AJ, Howe SD, Thomson AJ, Harrison KJ. Octa-Alkoxy Phthalocyanine and Naphthalocyanine Derivatives - Dyes with Q-Band Absorption in the Far Red or near-Infrared. *J Chem Soc, Perkin Trans* 1988;1:2453–2458.
25. Ogunsipe A, Nyokong T. Effects of central metal on the photophysical and photochemical properties of non-transition metal sulfophthalocyanine. *J Porphyrins Phthalocyanines* 2005;9:121–129.

26. Ogunsipe A, Nyokong T. Photophysical and photochemical studies of sulphonated non-transition metal phthalocyanines in aqueous and non-aqueous media. *J Photochem Photobiol, A* 2005;173:211–220.
27. Li XY, Ng DKP. Synthesis and spectroscopic properties of the first phthalocyanine-nucleobase conjugates. *Tetrahedron Lett* 2001;42:305–309.
28. Devlin R, Studholme RM, Dandliker WB, Fahy E, Blumeyer K, Ghosh SS. Homogeneous Detection of Nucleic-Acids by Transient-State Polarized Fluorescence. *Clin Chem* 1993;39:1939–1943. [PubMed: 8375078]
29. Walker GT, Nadeau JG, Linn CP, Devlin RF, Dandliker WB. Strand displacement amplification (SDA) and transient state fluorescence polarization detection of *Mycobacterium tuberculosis* DNA. *Clin Chem* 1996;42:9–13. [PubMed: 8565240]
30. Hammer RP, Owens CV, Hwang SH, Sayes CM, Soper SA. Asymmetrical, water-soluble phthalocyanine dyes for covalent labeling of oligonucleotides. *Bioconjugate Chem* 2002;13:1244–1252.
31. Koval VV, Chernonosov AA, Abramova TV, Ivanova TW, Fedorova OS, Derkacheva VM, Lukyanets EA. Photosensitized and catalytic oxidation of DNA by metallophthalocyanineoligonucleotide conjugates. *Nucleosides Nucleotides Nucleic Acids* 2001;20:1259–1262. [PubMed: 11562998]
32. Ogunsipe A, Nyokong T. Photophysicochemical consequences of bovine serum albumin binding to non-transition metal phthalocyanine sulfonates. *Photochem Photobiol Sci* 2005;4:510–516. [PubMed: 15986058]
33. Huang JD, Wang SQ, Lo PC, Fong WP, Ko WH, Ng DKP. Halogenated silicon(IV) phthalocyanines with axial poly(ethylene glycol) chains. Synthesis, spectroscopic properties, complexation with bovine serum albumin and in vitro photodynamic activities. *New J Chem* 2004;28:348–354.
34. Chen XL, Li DH, Zhu QZ, Yang HH, Zheng H, Wang ZH, Xu JG. Determination of proteins at nanogram levels by a resonance light-scattering technique with tetra-substituted sulphonated aluminum phthalocyanine. *Talanta* 2001;53:1205–1210. [PubMed: 18968214]
35. Peng X, Draney DR, Volcheck WM, Bashford GR, Lamb DT, Grone DL, Zhang Y, Johnson CM. Phthalocyanine dye as an extremely photostable and highly fluorescent near-infrared labeling reagent. *Proc SPIE Int Soc Opt Eng* 2006;6097:60970E/160970E/12.
36. Sibrian-Vazquez M, Ortiz J, Nesterova IV, Fernandez-Lazaro F, Sastre-Santos A, Soper SA, Vicente MGH. Synthesis and properties of cell-targeted Zn(II)-phthalocyanine-peptide conjugates. *Bioconjugate Chem* 2007;18:410–420.
37. Duan WB, Smith K, Savoie H, Savoie H, Greenman J, Boyle RW. Near IR emitting isothiocyanato-substituted fluorophores: their synthesis and bioconjugation to monoclonal antibodies. *Org Biomol Chem* 2005;3:2384–2386. [PubMed: 15976852]
38. Vrouenraets MB, Visser GWM, Stigter M, Oppelaar H, Snow GB, van Dongen G. Targeting of aluminum (III) phthalocyanine tetrasulfonate by use of internalizing monoclonal antibodies: Improved efficacy in photodynamic therapy. *Cancer Res* 2001;61:1970–1975. [PubMed: 11280754]
39. Carcenac M, Dorvillius M, Garambois V, Glaussel F, Larroque C, Langlois R, Hynes NE, van Lier JE, Pelegrin A. Internalisation enhances photo-induced cytotoxicity of monoclonal antibody-phthalocyanine conjugates. *Br J Cancer* 2001;85:1787–1793. [PubMed: 11742503]
40. Hammer, RP.; Soper, SA.; Pakhomov, S.; Jensen, TJ.; Allen, M.; Nesterova, IV.; Vicente, MDGH. Board of Supervisors of LA State University and Agricultural and Mechanical College, Application. WO 2007. p. 75
41. Koval VV, Chernonosov AA, Abramova TV, Ivanova TM, Fedorova OS, Knorre DG. The synthesis of a cobalt(II) tetracarboxyphthalocyanine-deoxyriboooligonucleotide conjugate as a reagent for the directed DNA modification. *Bioorg Khim* 2000;26:118–125. [PubMed: 10808407]
42. Deleted in proof.
43. Hermanson, GT., editor. *Bioconjugate Techniques*. 1995.
44. Yang YC, Ward JR, Seiders RP. Dimerization of cobalt(II) tetrasulfonated phthalocyanine in water and aqueous alcoholic solutions. *Inorg Chem* 1985;24:1765–1769.

45. Cox WG, Singer VL. Fluorescent DNA hybridization probe preparation using amine modification and reactive dye coupling. *Biotechniques* 2004;36:114–122. [PubMed: 14740493]
46. Lebedeva NS. Aggregation properties of water-soluble metal phthalocyanines: effect of ionic strength of solution. *Russ Chem Bull* 2004;53:2674–2683.
47. Li XY, He X, Ng ACH, Wu C, Ng DKP. Influence of surfactants on the aggregation behavior of water-soluble dendritic phthalocyanines. *Macromolecules* 2000;33:2119–2123.
48. Howe L, Zhang JZ. Ultrafast studies of excited-state dynamics of phthalocyanine and zinc phthalocyanine tetrasulfonate in solution. *J Phys Chem A* 1997;101:3207–3213.
49. Dhimi S, Demello AJ, Rumbles G, Bishop SM, Phillips D, Beeby A. Phthalocyanine Fluorescence at High-Concentration - Dimers or Reabsorption Effect. *Photochem Photobiol* 1995;61:341–346.
50. Ferencz A, Neher D, Schulze M, Wegner G, Viaene L, Deschryver FC. Synthesis and Spectroscopic Properties of Phthalocyanine Dimers in Solution. *Chem Phys Lett* 1995;245:23–29.
51. Boguta A, Wojcik A, Ion RM, Wrobel D. Photothermal methods as tools for investigation of weakly interacting non-fluorescent phthalocyanines. *J Photochem Photobiol, A* 2004;163:201–207.
52. Schutte WJ, Sluytersrehabach M, Sluyters JH. Aggregation of an octasubstituted phthalocyanine in dodecane solution. *J Phys Chem* 1993;97:6069–6073.
53. Flanagan JH, Khan SH, Menchen S, Soper SA, Hammer RP. Functionalized tricarbocyanine dyes as near-infrared fluorescent probes for biomolecules. *Bioconjugate Chem* 1997;8:751–756.
54. Dork T, Macek M, Mekus F, Tummler B, Tzountzouris J, Casals T, Krebsova A, Koudova M, Sakmaryova I, Macek M, Vavrova V, Zemkova D, Ginter E, Petrova NV, Ivaschenko T, Baranov V, Witt M, Pogorzelski A, Bal J, Zekanowsky C, Wagner K, Stuhmann M, Bauer I, Seydewitz HH, Neumann T, Jakubiczka S, Kraus C, Thamm B, Nechiporenko M, Livshits L, Mosse N, Tsukerman G, Kadasi L, Ravnik-Glavac M, Glavac D, Komel R, Vouk K, Kucinskas V, Krumina A, Teder M, Kocheva S, Efremov GD, Onay T, Kirdar B, Malone G, Schwarz M, Zhou ZQ, Friedman KJ, Carles S, Claustres M, Bozon D, Verlingue C, Ferec C, Tzetis M, Kanavakis E, Cuppens H, Bombieri C, Pignatti PF, Sangiuolo F, Jordanova A, Kusic J, Radojkovic D, Sertic J, Richter D, Rukavina AS, Bjorck E, Strandvik B, Cardoso H, Montgomery M, Nakielna B, Hughes D, Estivill X, Aznarez I, Tullis E, Tsui LC, Zielenski J. Characterization of a novel 21-kb deletion, CFTRdele2,3(21 kb), in the CFTR gene: a cystic fibrosis mutation of Slavic origin common in Central and East Europe. *Hum Genet* 2000;106:259–268. [PubMed: 10798353]
55. Michalet X, Pinaud FF, Bentolila LA, Tsay JM, Doose S, Li JJ, Sundaresan G, Wu AM, Gambhir SS, Weiss S. Quantum dots for live cells, in vivo imaging, and diagnostics. *Science* 2005;307:538–544. [PubMed: 15681376]



**Figure 1.** Electronic absorption (a) and emission (b) spectra of a cyanine dye, Cy7 (—), and ZnPc 2 (---). All spectra were acquired using the dyes at a concentration of approximately  $1 \mu\text{M}$  and placed in a DMSO solvent. The spectra were normalized to the absorption or emission maxima.

**Figure 2.**

Ion pair, reverse-phase chromatograms of reaction mixtures consisting of a ZnPc succinimidyl ester and an oligonucleotide along with control reactions consisting of the native ZnPc dye and an oligonucleotide. (a) Reactions with succinimidyl ester **4** (—, reaction with **C6-O1**; ---, **C12-O1**; ···, ZnPc **2**; ·-·-·, gradient composition). (b) Reaction with succinimidyl ester **4** and a control reaction with the native ZnPc dye (—, reaction with succinimidyl ester **4**; ···, reaction with ZnPc **2**; ·-·-·, gradient composition).

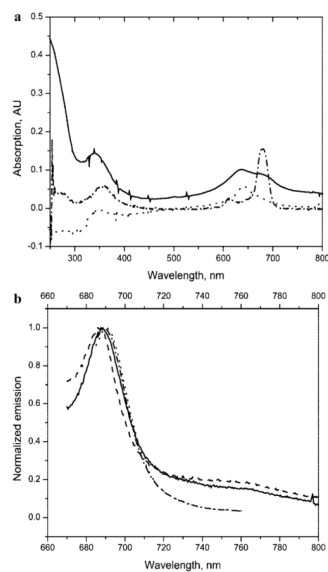


**Figure 3.** Absorption and emission spectra of purified conjugates and the native MPc dyes. (a) Electronic absorption spectra of **2** (2  $\mu$ M) in NH<sub>4</sub>OH (pH 11) (···), **2-C12-O1** (concentration unknown) in NH<sub>4</sub>OH (pH 11) (—), and **2** (2  $\mu$ M) in DMSO (·-·-·); (b) Fluorescence emission spectra ( $\lambda_{\text{ex}} = 650$  nm) of **1** (100 nM) in NH<sub>4</sub>OH at pH9/MeOH (50/50) (·-·-·), conjugate **1-C12-O1** (concentration unknown) in NH<sub>4</sub>OH at pH9/MeOH (50/50) (···), **2** (100 nM) in carbonate buffer at pH11/MeOH (50:50) (---) and **2-C12-O1** (concentration unknown) in carbonate buffer at pH11/MeOH (50:50) (—).

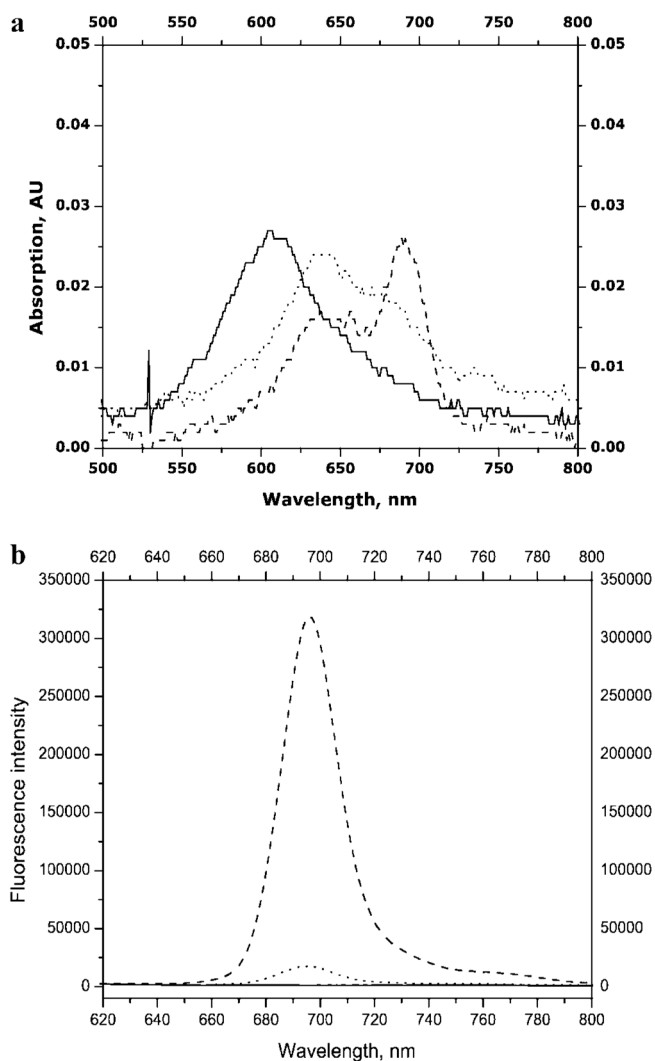


**Figure 4.** Absorption (a) and emission (b) spectra of solutions of ZnPc **2** (—), conjugate **2-C6-O1** (···), and the hybrid of **2-C6-O1** and **O2** (---). The spectra were measured in a buffer containing 10 mM Tris-HCl, 4 mM MgCl<sub>2</sub>, and 15 mM KCl at pH 8.5.

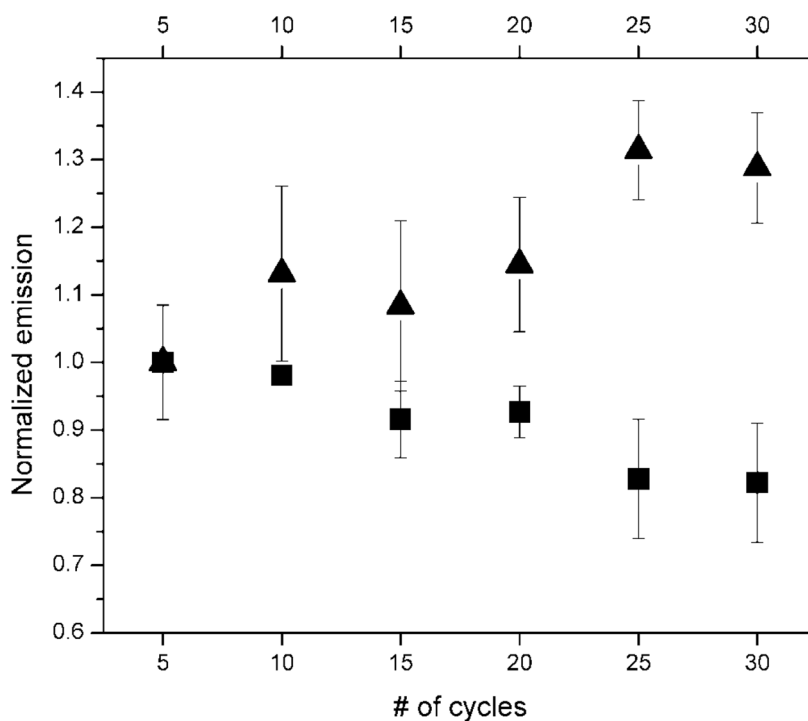


**Figure 5.** Fluorescence emission intensity of near-IR dye-labeled oligonucleotides (■, IRD700; ▲, ZnPc **2**) as a function of thermal cycle number. The reactions did not contain a target DNA or DNA polymerase. Thermal cycling conditions: 94 °C for 1 min; 55 °C for 40 s; 72 °C for 1 min. Emission wavelengths used were 700 nm for IRD700 and 690 nm for ZnPc **2**. Emission intensities were normalized to the intensity secured after 5 thermal cycles.

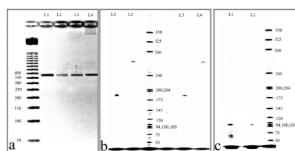
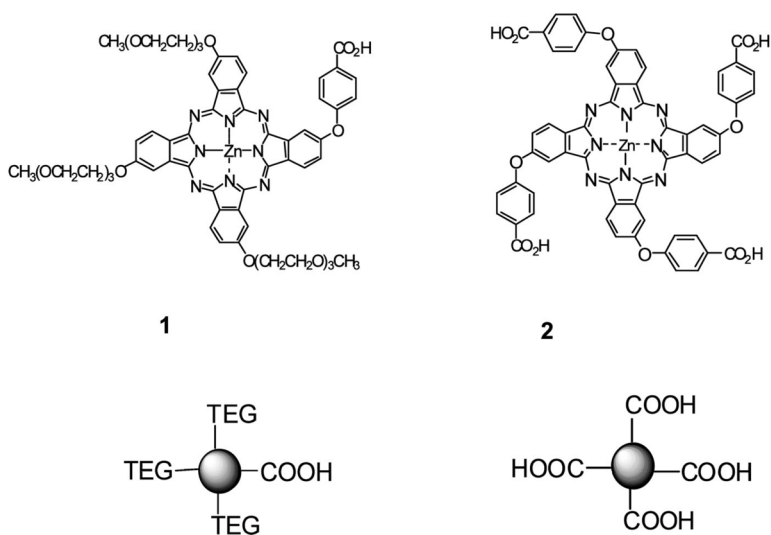
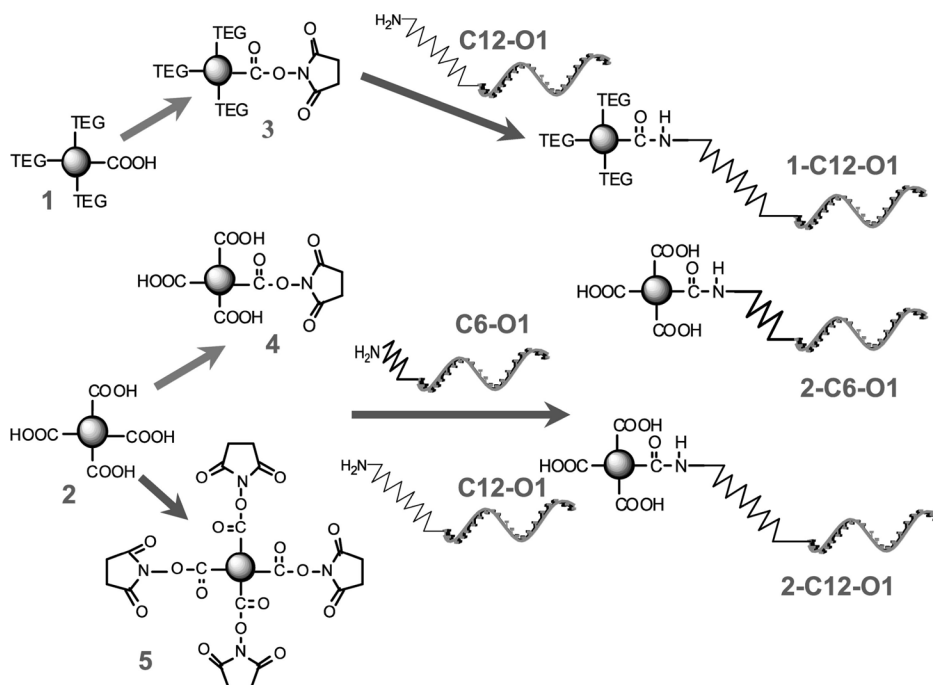


**Figure 6.**

Images of agarose (a) and polyacrylamide (b and c) gels after electrophoresis of PCR products. Detection was accomplished using UV absorption at 254 nm after staining the gel with ethidium bromide (a) or near-IR fluorescence at 700 nm (b and c). (a) 381 bp regions of M13mp18 amplified using primers **1-C12-O1** (L2), **2-C12-O1** (L3), **2-C6-O1** (L4), and unlabeled primer (L1). (b) 185 bp (L1, L3) and 272 bp (L2, L4) amplicons of a M13mp18 template amplified via PCR using primers **2-C6-O1** (L1, L2) or **1-C12-O1** (L3, L4). (c) (L1 and L2), 98 bp region of CFTR gene amplified via PCR using primer labeled with ZnPc **2**.



**Scheme 1.**  
Molecular Structures of the ZnPc's Used in These Studies



**Scheme 2.**  
 Conjugation Chemistries of ZnPc 1 and 2 and Their Corresponding Succinimidyl Esters to Oligonucleotide Targets

**Table 1**

Sequences of Oligonucleotides Used for Labeling Reactions, Hybridizations, and PCRs

oligos	sequence (5'→3')	$T_m$ (°C)
M13mp18 primer1 <sup>a</sup> ( <b>O1</b> )	GTA AAA CGA CGG CCA GT	52.6 °C
M13mp18 primer2 for 381 bp product	CAA CTC TCT CAG GGC CAG	55.0 °C
M13mp18 primer2 for 272 bp product	GGC CGA TTC ATT AAT GCA GC	54.8 °C
M13mp18 primer2 for 185 bp product	ACT CTA TAG GCA CCC CGA	54.2 °C
CFTR1 primer1 <sup>b</sup>	GTT GGC ATG CTT TGA TGA CGC TTC	59.4 °C
CFTR1 primer2	GTT TTC CTG GAT TAT GCC TGG GCA C	60.3 °C
Template 1 <sup>c</sup> ( <b>O2</b> )	<u>ACT GGC CGT CGT TTT ACA</u> ACG TCG TGA CTG GGA AAA	70.1 °C

<sup>a</sup>These primers were modified with an amino-group attached to its 5' end and were labeled with either ZnPc **1** (**1-C12-O1**, using a C<sub>12</sub>H<sub>24</sub> linker) or **2** (**2-C12-O1** or **2-C6-O1**, using a C<sub>12</sub>H<sub>24</sub> or C<sub>6</sub>H<sub>12</sub> linker, respectively).

<sup>b</sup>This primer was modified with an amino-group attached to its 5' end via a C<sub>6</sub>H<sub>12</sub> linker and was labeled with ZnPc **2**.

<sup>c</sup>The underlined sequence is complementary to **O1**.

**Table 2**

Estimated Labeling Efficiencies at Different MPc/oligonucleotide Molar Concentration Ratios Using Different Dyes, Linkers, and Succinimidyl Esters<sup>a</sup>

Linker <sup>b</sup>	MPc	succinimidyl ester	MPc/oligonucleotide	labeling efficiency
C <sub>12</sub> H <sub>24</sub>	1	3	5:1	<5%
C <sub>12</sub> H <sub>24</sub>	1	3	10:1	24 ± 6%
C <sub>12</sub> H <sub>24</sub>	1	3	18:1	48 ± 2%
C <sub>12</sub> H <sub>24</sub>	2	5	11:1	78 ± 5%
C <sub>12</sub> H <sub>24</sub>	2	5	21:1	56 ± 3%
C <sub>12</sub> H <sub>24</sub>	2	5	38:1	39 ± 2%
C <sub>6</sub> H <sub>12</sub>	2	4	1:1	<5%
C <sub>6</sub> H <sub>12</sub>	2	4	4:1	28 ± 3%
C <sub>6</sub> H <sub>12</sub>	2	4	9:1	38 ± 6%
C <sub>12</sub> H <sub>24</sub>	2	4	1:1	33 ± 6%
C <sub>12</sub> H <sub>24</sub>	2	4	4:1	47 ± 3%
C <sub>12</sub> H <sub>24</sub>	2	4	11:1	53 ± 4%

<sup>a</sup> Conjugation reactions were performed in borate buffer at pH 8.5 and using an oligonucleotide concentration of 20 nM.

<sup>b</sup> The aliphatic linker used to attach the amino group to the 5' end of the oligo-nucleotide.

**Table 3**Labeling Efficiencies of an Oligonucleotide with ZnPc 2 at Different Buffer and pH Conditions<sup>a</sup>

pH	borate	carbonate
7.5		67 ± 2%
8.0	26 ± 3%	
8.5	38 ± 6%	59 ± 2%
9.5	15 ± 1%	36 ± 2%

<sup>a</sup>The conjugation reactions used a C<sub>6</sub>H<sub>12</sub> linker, ZnPc 2, succinimidyl ester 4, and an MPc/oligonucleotide molar ratio of 9:1.